Strojniški vestnik - Journal of Mechanical Engineering 62(2016)2, 137-144
DOI:10.5545/sv-jme.2015.2994
Original Scientific Paper
Received for review: 2015-09-03
Received revised form: 2015-11-30
Accepted for publication: 2015-12-21

WEDM Manufacturing Method for Noncircular Gears, Using CAD/CAM Software

César García-Hernández[1,*] – Rafael-María Gella-Marín[1] – José-Luis Huertas-Talón[1] – Nikolaos Efkolidis[1] – Panagiotis Kyratsis[2]

[1] University of Zaragoza, Department of Design and Manufacturing Engineering, Spain
[2] Technological Education Institution of Western Macedonia, Department of Mechanical Engineering & Industrial Design, Greece

Noncircular gears are used in several technological applications in order to enhance the performance of different mechanical instruments (flow meters, bikes, internal combustion engines, etc.), in order to unify speed in assembly lines and in research. Noncircular gears are typically manufactured by shaving: milling each tooth or by generation. This requires controlling the geometric and kinematic variables in the process.

In this research, a method to manufacture elliptical and oval gears using wire electro-discharge machining (WEDM) is presented. This is a continuous procedure, and its performance is not inferior to the previously mentioned methods. Mathematical models for manufacturing elliptical and oval gears are presented, simulations are carried out, and this method is implemented in a WEDM machine, obtaining two pairs of elliptical and oval gears. This method could be useful in the manufacturing of injection moulds or custom-made metallic gears.

Finally, a discussion using bibliographic references is presented about the surface finish and the consequences of using WEDM in comparison to other shaving methods which do not involve a material phase change.

Keywords: WEDM, noncircular gears, worksheet, CAD/CAM

Highlights

- *Wire Electro Discharge Machining is applied to noncircular gear manufacturing.*
- *The mathematical models for manufacturing elliptical and oval gears are included.*
- *The algorithm of the mathematical models is implemented using MatlabTM.*
- *Simulations are carried out, and the method is implemented in a real WEDM machine.*
- *Two pairs of elliptical and oval gears are obtained applying this method.*

0 INTRODUCTION

The manufacture of noncircular gears (in which elliptical and oval gears are included) is an interesting research topic from several aspects.

It has practical commercial applications, since these gears are used in several mechanisms [1], such as in flow meters, chain transmission systems, transmissions of bike plates [2], oil pumps and even in chain belts used in combustion engines [3] (Fig. 1).

Noncircular gears are also studied as a way of developing different types of gears that can meet movement specifications [4] or as a way of experimenting with several machining methods [5].

They have also been used to transmit movement in several different ways, as we can see in different museums [6].

Similarly, this field has been addressed in research. In [7] a literature review is carried out, analysing the analytical methods used to obtain the equations which define the pitch circumference. Furthermore, the methods to obtain these gears are revised, and an experimental analysis is carried out of the transmission ratio relating to speed and torque.

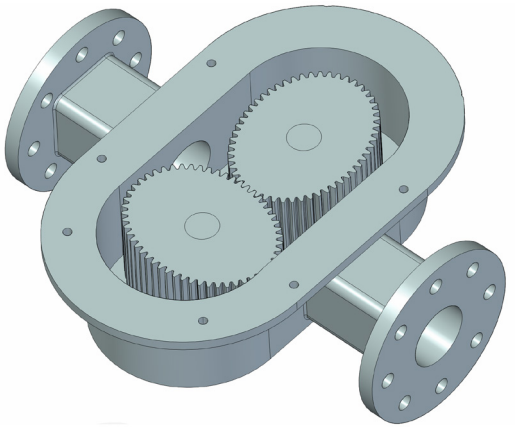

Fig. 1. *Flowmeter and oval gears*

It is important to point out the kinematic differences between noncircular gears. This research focuses on designing and manufacturing elliptical and oval gears. As it has been widely described [8], elliptical gears rotate around their focus.

*Corr. Author's Address: University of Zaragoza, Dept. of Design and Manufacturing Engeenering, Campus Río Ebro, C/ María de Luna, 3 - 50018 – Zaragoza, Spain, garcia-hernandez.cesar@unizar.es

However, this kinematic relation is not the same in oval gears. According to Bloomfield [9], two oval gears mesh when they rotate around their centre.

For this reason, this research addresses the development procedures in order to design and manufacture elliptical gears and oval gears. Even though two different methods are addressed to develop such gears, a common flowchart has been developed to organize the process. It is described in Fig. 2.

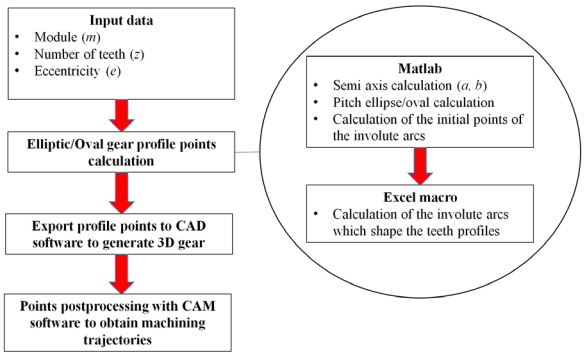

Fig. 2. *Flow chart for design and manufacturing*

According to this flowchart, the designing process is arranged using Matlab™ and an Excel™ macro. Starting from the initial input data, Matlab™ is used to calculate the semi-axis, the pitch ellipse/oval, and the initial points distributed on it from where the involute arcs define the start of the teeth. Then, a macro is used to calculate the involute arcs that define the teeth profiles. These points define the gear, and they are exported to general purpose CAD software [10] in order to obtain the 3D gear model; afterwards, they are post-processed in a CAM software to obtain the milling trajectories required to manufacture the gear. Elliptical and oval gears may be similar, but their behaviour is not the same, not only from a geometrical aspect but also from a kinematic point of view as described below.

In this article, a Cartesian coordinate system is used in the elliptical gear case and a polar coordinate system to develop the oval one. Being a and b, the semi-major and the semi-minor axes respectively, elliptical gears rotate with respect to their focuses and oval gears rotate around their centres. These differences, along with the equations describing the pitch ellipse and the pitch oval, are represented in Figs. 3 and 4, as shown below.

Elliptical gears rotating with respect to their focuses (Fig. 3):

$$\frac{x^2}{a^2}+\frac{y^2}{b^2}=1. \tag{1}$$

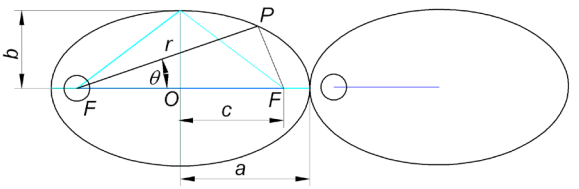

Fig. 3. *Elliptical gears*

Oval gears rotating with respect to their focuses (Fig. 4):

$$r=\frac{2ab}{(a+b)-(a-b)\cos 2\theta}. \tag{2}$$

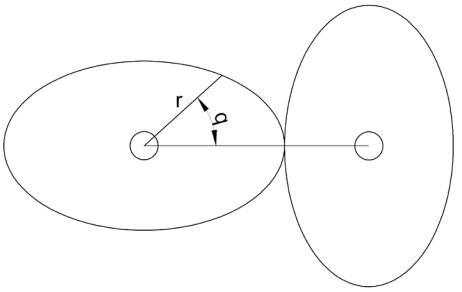

Fig. 4. *Oval gears*

1 METHODS

The procedure presented in this paper approaches the design by approximating and calculating the teeth as in the spur gears, but taking into account the local curvature of the ellipse [11] and the oval. In order to obtain the teeth of the gears, the radius of curvature of Eqs. (3) and (4) can be applied. It is expressed in Cartesian and polar coordinates respectively by [12]:

$$\rho=\frac{\left[1+\left(\frac{dy}{dx}\right)^2\right]^{3/2}}{\frac{d^2y}{dx^2}}, \tag{3}$$

$$\rho=\frac{\left[r^2+\left(\frac{dr}{d\theta}\right)^2\right]^{\frac{3}{2}}}{r^2+2\left(\frac{dr}{d\theta}\right)^2-r\frac{d^2r}{d\theta^2}}. \tag{4}$$

For the ellipse Eq. (1), applying Eq. (3), the radius of curvature in Cartesian coordinates is:

$$\rho=-\frac{\left[a^4y^2+b^4x^2\right]^{3/2}}{a^4b^4}. \tag{5}$$

As an example, the extreme values of the radius of curvature, for a = 100 and b = 60, are represented in Fig. 5.

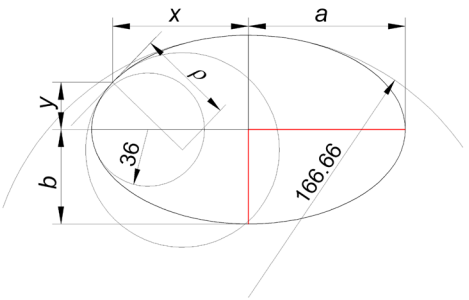

Fig. 5. *Extreme radii of curvature of an ellipse using Eq. (1)*

The radius of curvature obtained for the oval Eq. (2), as a result of applying Eq. (4), is a complex expression.

It is important to note that the oval Eq. (2) presents points with zero slope. When $a \leq 2b$ its aspect is similar to an ellipse. For greater values of the parameter a, six points with zero slope are obtained, Fig. 6a. In Fig. 6b, the maximum and the minimum radii of curvature are represented for $a=100$ and $b=60$.

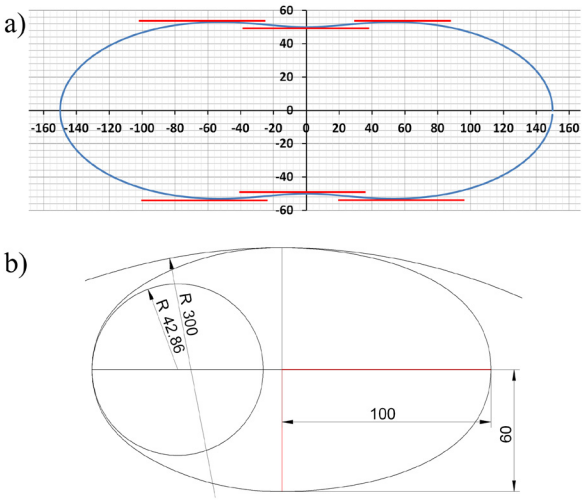

Fig. 6. *Different ovals; a) with a > 2b, and b) with a = 100 and b = 60*

In the intersection point of the symmetry axis of the tooth with the ellipse/oval, the constructive radius of this tooth is considered the radius of curvature of the pitch ellipse/oval in order to generate the tooth, Fig. 7.

The following considerations must also be taken into account.

The tooth thickness measured in the pitch ellipse/oval must be the same for all the teeth; otherwise, the teeth would not mesh with the hole between the flanks of consecutive teeth. As the final thickness is always lower than the nominal one, there is a bigger space between consecutive teeth.

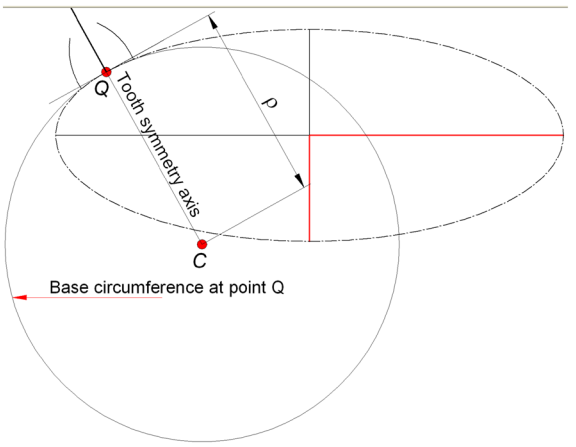

Fig. 7. *The tooth of the ellipse/oval corresponds to the tooth of a circle with the same curvature*

In a pair of gears, each one has z teeth, and a tooth pitch measured on the ellipse/oval of $p=\pi \cdot m$ (where m is the module), which is the double of the tooth thickness.

If the tooth pitch in the pitch ellipse/oval is $\pi \cdot m$, then the perimeter is $\pi \cdot m \cdot z$, this last value being the pitch ellipse/oval length.

In this case, the calculation starts using the pitch ellipse/oval length, obtaining the values of a and b through another condition, such as the eccentricity. In this way, if a gear with module m = 2.5, teeth number z = 53 and eccentricity e = 0.85 is manufactured, the ellipse/oval length is $l = \pi \cdot m \cdot z = \pi \cdot 2.5 \cdot 53 = 416.2610$. In order to obtain simpler values of a and b, another non-conventional module can be applied.

Here, two different methods are discussed to obtain the semi-axis a and b. They are not the same because different approaches are used with an ellipse and an oval, as follows.

1.1 Semi-axis a and b, calculation in an Ellipse

The ellipse length is obtained applying this integral:

$$l = 4\int_0^a \sqrt{d\,x^2 + d\,y^2}\,. \tag{6}$$

Solving Eq. (6) leads to an elliptic integral of the second order. After evaluating it with Matlab™ and equalizing it to the value of the ellipse perimeter, it is

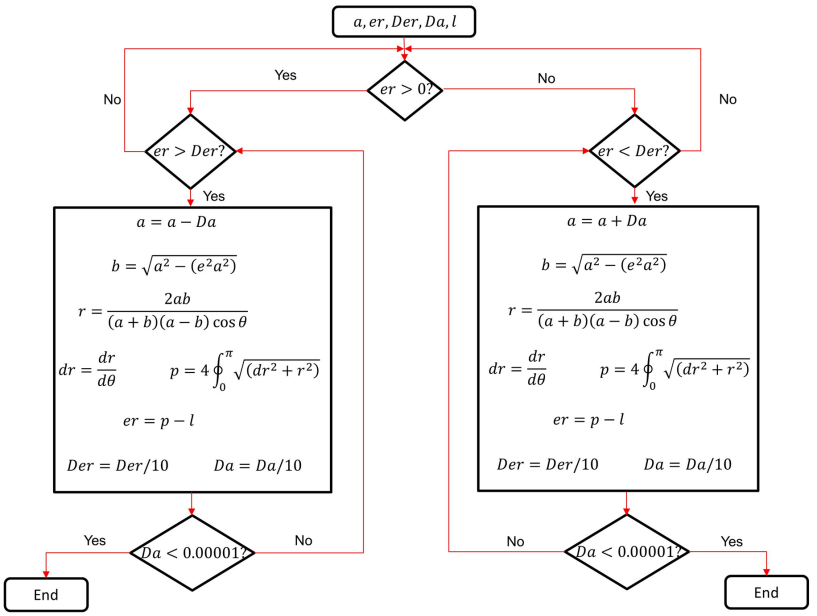

Fig. 8. *Numerical method to obtain semi-axis a and b, solving Eq. (7)*

possible to solve it and to obtain the value of the semi-axis a and b.

1.2 Semi-axis a and b, Calculation in an Oval

The oval length is obtained applying the integral:

$$l = 4\int_0^{\frac{\pi}{2}} \sqrt{\left(\frac{dr}{d\theta}\right)^2 + r^2}\, d\theta. \tag{7}$$

It is not possible to solve this equation directly with Matlab™; numerical methods can be applied in order to evaluate the integral and equalize it to the value of the oval perimeter with an error smaller than the value set by the gear designer.

The numerical method to obtain the value of the semi-axis a and b is presented in Fig. 8.

Table 1. *Uncertainties in the algorithm*

l	Oval perimeter calculated with the input data
a	Major semi-axis
b	Minor semi-axis
E	Eccentricity
er	Error between the calculated perimeter by the numerical method and by the input data
r	Oval polar equation
p	Oval perimeter calculated by integration
Der	Error increment between iterations
Da	Value to decrement or increment the semi-major axis initial value between iterations

The uncertainties in the algorithm are summarized in Table 1. In this algorithm, the initial values for the major and the minor semi-axis a and b are considered. The perimeter value is calculated using input data. Then, using the algorithm, the initial value of the major semi-axis a is increased or decreased until the difference between the perimeter calculated using these values and the perimeter obtained from the input data is smaller than a given error.

1.3 Tooth Distribution

A starting point for the pitch ellipse/oval (Fig. 9) is chosen, in this case (a, 0), and the points of the pitch ellipse or the pitch oval are calculated. The calculation of the teeth distribution starts with a Matlab™ program and ends with an Excel™ macro.

The Matlab™ program determines the pitch ellipse points with a chordal error lower than a given value, Fig. 6.

In the environment of point $A(x_1, y_1)$, point $B(x_2, y_2)$ is obtained satisfying the condition that the secant AB maintains a maximum distance d to the curve. This distance is obtained by substituting the coordinates $T(x_3, y_3)$ in the normal equation of the line.

$$d = \frac{a \cdot x_3 + b \cdot y_3 + c}{\sqrt{a^2 + b^2}}. \tag{8}$$

The sign of the distance d must also be kept in mind, which indicates the semiplane where the point

taken as a reference for that distance is placed. In this case, the square of the distance has been evaluated in order not to take into consideration the distance sign.

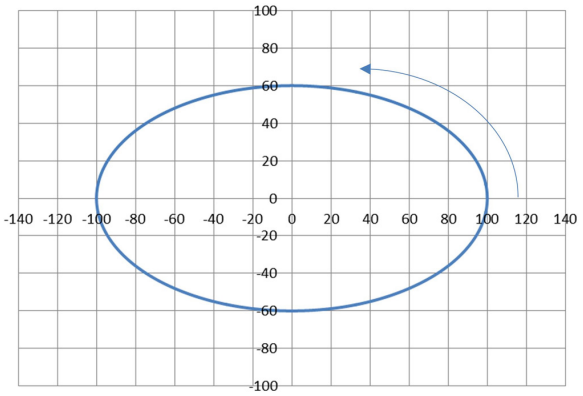

Fig. 9. *Pitch ellipse*

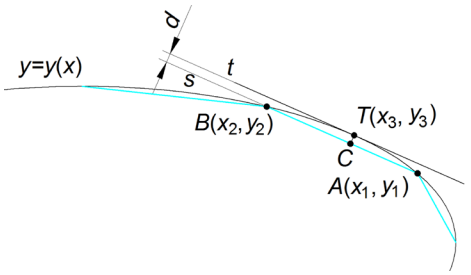

Fig. 10. *Obtaining the ellipse points*

$$d^2 = \frac{\left(a \cdot x_3 + b \cdot y_3 + c\right)^2}{\left(a^2 + b^2\right)}. \tag{9}$$

The point T is the point of tangency of the parallel line to the secant segment AB with the function graph. Therefore, the first derivate in T is equal to the tangent of the α angle.

$$y'_{x=x_3} = \frac{y_2 - y_1}{x_2 - x_1}. \tag{10}$$

In this way, the two conditions which will allow solving the two uncertainties (x_2, y_2) are found.

It is not necessary to analyse the sign of the tangent, because the trajectory is known. In order to solve this system of two equations with numerical methods, MATLAB™ makes possible the application of the following command [13]:

```
maple(fsolve({equ1,equ2},{var1,var2},{var1=v1initial..
v1final,var2=v2initial..v2final}))
```

Knowing the tooth thickness, the ellipse arc segments of the calculated length are distributed on the ellipse and the radius of curvature of these points are determined (Fig. 11).

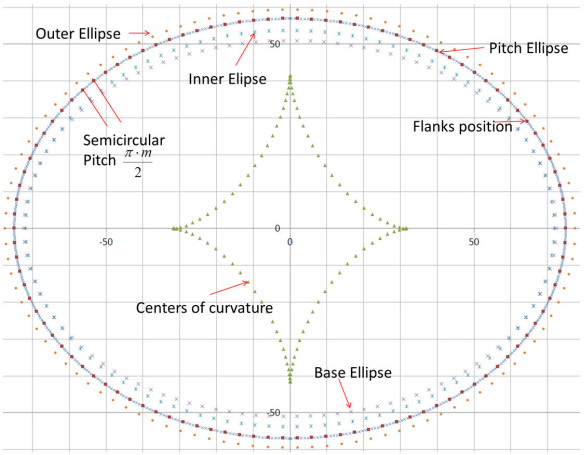

Fig. 11. *Points to position the flanks and other characteristic points*

In order to obtain the initial points of the involute arcs, that the ellipse/oval length obtained by Eqs. (6) and (7) lead to elliptical integrals must be taken into account. For this reason, these calculations have been carried out in MATLAB™, but once the points of the pitch ellipse have been obtained, the separation value of the half tooth pitch is calculated, finding the points that have a separation of this value between them. The following equation is used:

$$l = \sum \sqrt{\left(x_{i+1} - x_i\right)^2 + \left(y_{i+1} - y_i\right)^2}. \tag{11}$$

When the length is greater than the tooth thickness on the pitch ellipse/oval, an additional point is interpolated, and this additional point becomes a part of the series of points of the linear approximation (Fig. 12).

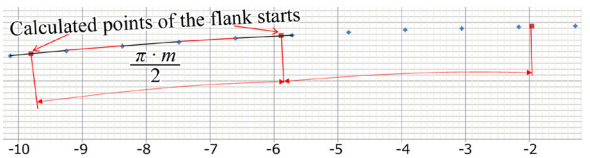

Fig. 12. *Starting flank points calculated on the pitch ellipse/oval*

The absolute error, which is obtained on a perimeter of 416.2589, is smaller than 0.0021 for a chordal error below 0.001.

On these points, the involute arcs corresponding to the radius of the local curvature have been placed (Fig. 13). These arcs start from the base ellipse/oval (equivalent to the base circumference of the local radius of curvature), and have been extended beyond

the exterior ellipse/oval. The real tooth will be located between the interior and the exterior ellipse/oval. However, it must be taken into account that not all the teeth can reach the bottom of the calculated involute profile, because when there is a low number of local teeth, where the curvature is smaller, the inner locally equivalent diameter is bigger than the base one.

This involute profile, Fig. 13b, has been calculated as in reference [14], but using an Excel™ macro, as it is possible to export the Excel™ data to a general purpose CAD software. In this case, the command "curve by table" of Solid Edge has been used. This process can be automated with a Visual Basic macro [15]. This command also makes it possible to export the points of the addendum, dedendum, and pitch ellipses/ovals.

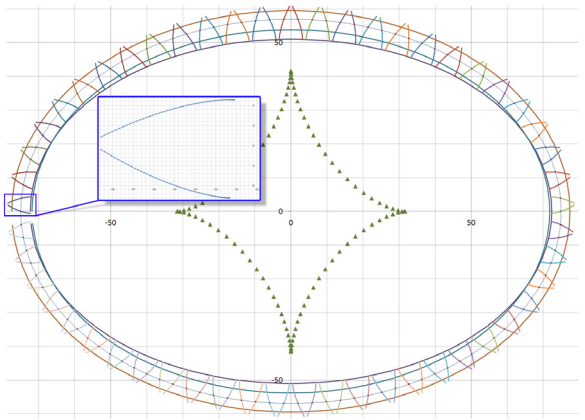

Fig. 13. *Points of the different involutes according to the radius of curvature*

2 EXPERIMENTAL MANUFACTURING PROCESS

Once all these curves have been exported to Solid Edge, the correspondent extrusions and the rounding of the teeth fillet are carried out (Figs. 14 and 15).

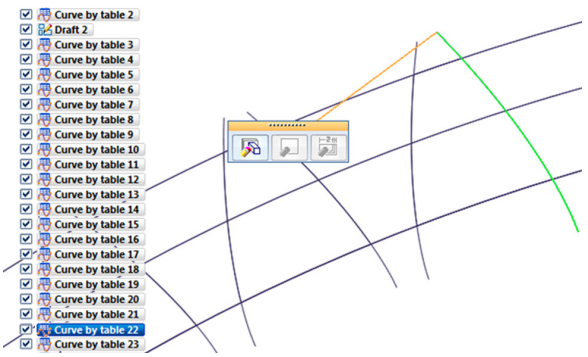

Fig. 14. *Calculated points imported in Solid Edge™*

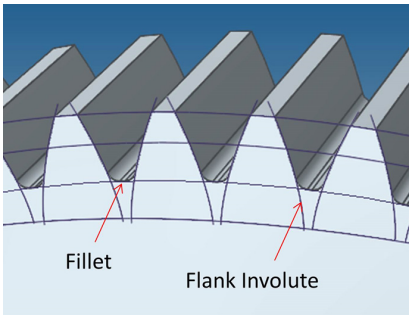

Fig. 15. *Extrusions and fillets*

All these operations could have been carried out directly with Excel™ or Matlab™, calculating the position of the rounding points for each tooth, as described in [14]. The continuity of the points of the dedendum, addendum, and the flank points, which correspond to a specific tooth profile, provide the path of the WEDM. A wire radius correction plus a gap is applied to these points. However, in this case, general purpose CAD software was used in the process and, later, CAM software was applied. As an example, EdgeCAM™ [16] has been used to make a pair of gears with an eccentricity of 0.75 and 80 teeth are shown.

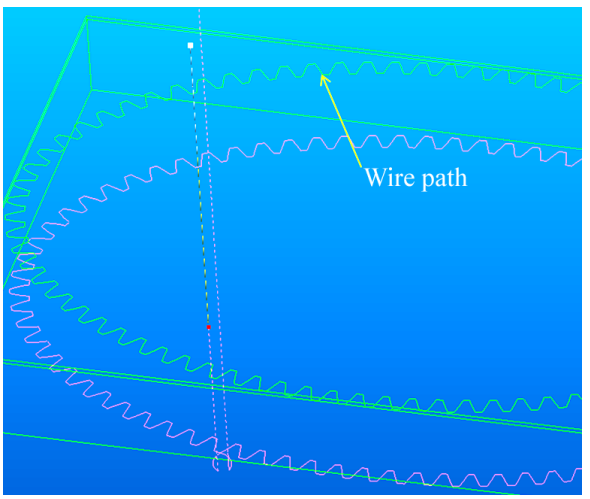

Fig. 16. *Points post-processed in a CAM software*

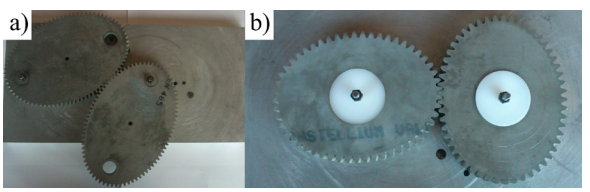

Fig. 17. *Two manufactured gears; a) elliptical; b) oval*

3 RESULTS AND DISCUSSION

The method presented in this work does not use machines dedicated to a specific manufacturing process, such gear-milling machines, using universal-purpose programmable machines. The technology applied involves a phase shift to obtain the chip removal, which can originate some problems in certain materials.

In previous research [17] and [18], a miniature brass gear was manufactured with WEDM, and the advantages of using this method were analysed. Those papers described the obtained results and analysed the superficial parameters of microhardness and microstructure, concluding that this method is appropriate to obtain good quality levels (N5). In the case of steel, surface quality and fatigue studies were carried out using high alloy steel for manufacturing tools, applying WEDM [19], demonstrating that an adequate selection of parameters is needed for an optimum WEDM finishing.

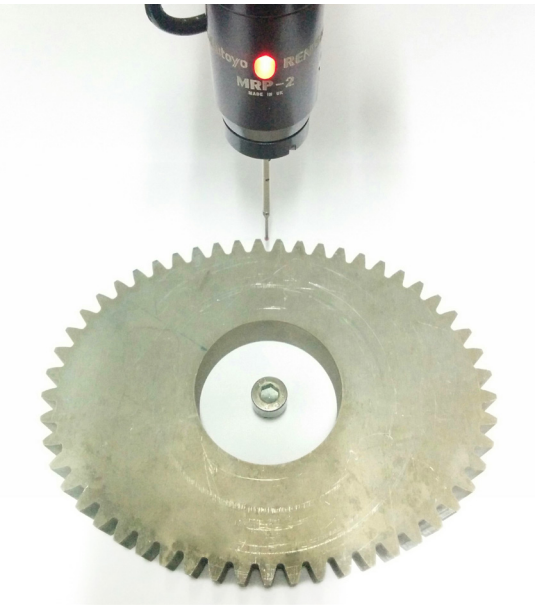

Fig. 18. *Validation of the algorithm with a coordinate measuring machine*

In different research [20], the same conclusions were reached with Inconel 718. The superficial finishing was very good, but the conditions of intensity, pulse and discharge time must be taken into consideration in order to obtain a superficial microstructure that does not damage the future integrity of the manufactured part. However, there are previous works [21] in which it was shown that WEDM involves a roughness increase and a decrease of fatigue resistance, in comparison to test pieces manufactured with turning processes. The discrepancy of these results was explained by the difference of twelve years between the machines used for the experimental works ([21] vs. [22]). During this time, manufacturers applied technological improvements to their machines [22]. This is congruent with the conclusions obtained in [23] for Ti–6Al–4V alloy.

The algorithm was validated by measuring the eroded teeth with a coordinate measuring machine (Fig. 18). These gears had a tolerance value better than 5 μm, between the maximum and minimum profiles of the manufactured involute, so the manufactured gear offers optimum quality.

4 CONCLUSIONS

Even though the application field of elliptical/oval gears is not very extensive, it can be very convenient when a non-constant torque must be transmitted, as well as for research. Simplifying the gear manufacturing process without specific machinery, makes the processes of research, design, and manufacture more accessible to a larger number of people. The example described in this study has been generalized to obtain machining paths, using CAM software. The use of CAM allows manufacturing with several methods: WEDM, water jet cut, laser cut, milling, etc. In this way, a good method is presented so the developer can control the gear design and also the manufacturing methods which ensure a better gear finishing. Although MATLAB™ has been used to solve the equations, it is also possible to apply Excel™, implementing numerical methods with a macro.

Finally, with the analysed references about the obtained superficial features in the process, it can be concluded that, with the available machinery and an optimum selection of the conditions which define the process, e.g. intensity, pulse time, etc. (paying attention to the manufacturer advice), the obtained metrological, physical and chemical properties are similar to any other manufacturing process.

5 REFERENCES

[1] Hebbale K, Li D, Zhou J, Duan C, Kao C.K., Samie, F., Lee, C., Gonzales, R. (2014). Study of a non-circular gear infinitely variable transmission. *ASME 2014 Dynamic Systems and Control Conference*, paper no. DSCC2014-6083, p. V003T49A003, **DOI:10.1115/dscc2014-6083**.

[2] Bini, R.R., Dagnese, F. (2012). Noncircular chainrings and pedal to crank interface in cycling: a literature review.

Brazilian Journal of Kinantrophometry and Human Performance, vol. 14, no. 4, p. 470-482, **DOI:10.5007/1980-0037.2012v14n4p470**.

[3] Volkswagen (2015). from *www.volkspage.net/technik/ssp/ssp/SSP_337.pdf*, accessed on 2015-04-06.

[4] Litvin, F.L., Gonzalez-Perez, I., Fuentes, A., Hayasaka, K. (2008). Design and investigation of gear drives with non-circular gears applied for speed variation and generation of functions. *Computer Methods in Applied Mechanics and Engineering*, vol. 197, no. 45-48, p. 3783-3802, **DOI:10.1016/j.cma.2008.03.001**.

[5] Li, J., Wu, X., Mao, S. (2007). Numerical computing method of noncircular gear tooth profiles generated by shaper cutters. *The International Journal of Advanced Manufacturing Technology*, vol. 33, no. 11-12, p. 1098-1105, **DOI:10.1007/s00170-006-0560-0**.

[6] Efstathiou, K., Basiakoulis, A., Efstathiou, M., Anastasiou, M., Seiradakis, J.H. (2012). Determination of the gears geometrical parameters necessary for the construction of an operational model of the Antikythera Mechanism. *Mechanism and Machine Theory*, vol. 52, p. 219-231, **DOI:10.1016/j.mechmachtheory.2012.01.020**.

[7] Quintero Riaza H.F. (2014). from *http://www.tdx.cat/handle/10803/6418*, accessed on 2014-04-06.

[8] Litvin, F.L., Fuentes, A. (2004). *Gear Geometry and Applied Theory.* Cambridge University Press, Cambridge, **DOI:10.1017/CBO9780511547126**.

[9] Bloomfield, B. (1960). *Noncircular Gears*. Product Engineering Special Report; p. 159-165.

[10] Haba, S.A., Oancea, G. (2015). Digital manufacturing of air-cooled single-cylinder engine block. *The International Journal of Advanced Manufacturing Technology*, vol. 80, no. 5, p. 747-759, **DOI:10.1007/s00170-015-7038-x**.

[11] Fuentes-Aznar, A., Gonzalez-Perez, I., Hayasaka, K. (2009). *Noncircular gears: Design and Generation*. Cambridge University Press, Cambridge, p. 36-37 and p. 47-52.

[12] Mataix, C.M. (1967). *Análisis algébraico e infinitesimal.* Editorial Nuevas Graficas, Madrid. (in Spanish)

[13] del Río, J.A.I., Cabezas, J.M.R. (2007). *Métodos Numéricos: Teoría, problemas y prácticas con Matlab™* (eng: Numerical Methods: Theory, problems and practice with Matlab ™). Ed. Pirámide, Madrid. (in Spanish)

[14] Talón, J.L.H., Ortega, J.C.C., Gómez, C.L., Sancho, E.R., Olmos, E.F. (2010). Manufacture of a spur tooth gear in Ti–6Al–4V alloy by electrical discharge. *Computer-Aided Design*, vol. 42, no. 3, p. 221-230, **DOI:10.1016/j.cad.2009.11.001**.

[15] Siemens. (2015). Solid Edge "Programming User's Guide" Version 1.0 and 2.0, Plano.

[16] Vero Software (2015). f*rom www.edgecam.com*, accessed on 2015-04-06.

[17] Gupta, K., Jain, N.K. (2014). Comparative study of wire-EDM and hobbing for manufacturing high-quality miniature gears. *Materials and Manufacturing Processes*, vol. 29, no. 11-12, p. 1470-1476, **DOI:10.1080/10426914.2014.941865**.

[18] Gupta, K., Jain, N.K. (2014). On surface integrity of miniature spur gears manufactured by wire electrical discharge machining. *The International Journal of Advanced Manufacturing Technology*, vol. 72, no. 9-12, p. 1735-1745, **DOI:10.1007/s00170-014-5772-0**.

[19] Ghanem, F., Fredj, N.B., Sidhom, H., Braham, C. (2011). Effects of finishing processes on the fatigue life improvements of electro-machined surfaces of tool steel. *The International Journal of Advanced Manufacturing Technology*, vol. 52, no. 5-8, p. 583-595, **DOI:10.1007/s00170-010-2751-y**.

[20] Li, L., Guo, Y.B., Wei, X.T., Li, W. (2013) Surface integrity characteristics in wire-EDM of Inconel 718 at different discharge energy. *Procedia CIRP*, vol. 6, p. 220-225, **DOI:10.1016/j.procir.2013.03.046**.

[21] Ferrer, C., Cárcel, A., Pascual-Guillamón, M., Pérez-Puig, M.A., Segovia, F., Razzaq, K.A. (2003). *Investigación de las causas que modifican la resistencia a fatiga en flexión rotativa del proceso de mecanización de electroerosión por hilo en las aleaciones de aluminio AA-2000* (eng. *Research of the causes that modify the fatigue resistance in rotated flexion of the process by wire electro discharge machining in the aluminum alloys AA-2000*). *Anales de mecánica de la fractura* (eng. *Annals of Fracture Mechanics*), vol. 20, p. 201-206. (in Spanish)

[22] Ona Electroerosión (2015). *from www.ona-electroerosion.com,* accessed on 2015-04-06.

[23] Mower, T.M. (2014). Degradation of titanium 6Al–4V fatigue strength due to electrical discharge machining. *International Journal of Fatigue*, vol. 64, p. 84-96, **DOI:10.1016/j.ijfatigue.2014.02.018**.